Segment diffusion and flip-flop spin diffusion in entangled polyethyleneoxide melts: A field-gradient NMR diffusometry study

Elmar Fischer and Rainer Kimmich
Sektion Kernresonanzspektroskopie, Universität Ulm, 89069 Ulm, Germany

Nail Fatkullin and Galina Yatsenko
Kazan State University, 420008 Kazan, Russia

(Received 1 April 1999; revised manuscript received 7 January 2000)

Chain dynamics in melts of entangled polyethyleneoxide melts has been investigated using fringe field nuclear magnetic resonance diffusometry. As already demonstrated in our previous work, intermolecular flip-flop spin diffusion strongly influences spin echo attenuation for long diffusion times and high molecular weights. The experimental data have been evaluated taking this phenomenon quantitatively into account. Predictions of the reptation model for the correspondingly modified time and molecular weight dependences of the effective segment diffusion coefficient are presented and compared with experimental results. While the ordinary Rouse model totally fails to explain the experimental data, a satisfactory qualitative description is provided on the basis of the tube/reptation model. However, the fitted parameter values turned out to be inconsistent with known properties of this polymer. This in particular refers to the mean squared chain end-to-end distance divided by the molecular weight, for which neutron-scattering values are available in the literature. Relative to those results, the value evaluated from our NMR diffusometry data on the basis of the tube/reptation model turned out to be much too large.

PACS number(s): 61.25.Hq, 66.10.Cb

I. INTRODUCTION

The anomalous characteristics of segment diffusion in melts of entangled polymers such as the time and molecular-weight dependences of the effective diffusion coefficient are indicative for the type of dynamics the polymer chains exhibit. Field gradient NMR diffusometry (FGD) [1] and in particular the fringe-field version of it therefore are of interest as suitable tools for corresponding studies.

As shown in our previous paper [2] and verified in the work of another group [3], spins are not only displaced by segment diffusion in the sense of Brownian motion. At diffusion times t long enough and high molecular masses M, immaterial displacements in the form of spin flip-flops of dipolar coupled spin pairs come into play, and may even dominate the spin displacements of spins. Pairs of dipolar coupled spins perform mutual flips. One coupling partner changes its state from spin-down to spin-up whereas the other performs the opposite transition. A series of such flip-flop processes effectively leads to a spin transport competing with the Brownian displacement of the spin bearing nuclei. The efficiency of this immaterial transport process is a question of the strength of dipolar coupling and of the diffusion time. Melts of polymers with molecular masses far above the critical value M_c are characterized by slow chain dynamics so that motional averaging of dipolar couplings is weak. The mean flip-flop time τ_{ff} in such melts was estimated [2] to be of the order 100 ms. That is, flip-flop spin diffusion must be taken into account in entangled polymer systems at diffusion times longer than 100 ms. On the other hand, on a shorter time scale or for molecular masses close to or below the critical value, spin echo attenuation will be dominated by the true Brownian displacement of segments.

Note that the crossover between the regimes where the two mechanisms start to dominate is relatively sharp: Decreasing the molecular mass strongly enhances Brownian diffusion while dipolar coupling is more efficiently averaged out so that flip-flop spin diffusion is diminished, and vice versa. There are two displacement mechanisms acting in opposite directions. Temperature variation as far as possible in polymer melts without degradation on the one hand and glass transition on the other is of minor influence. In particular, flip-flop spin diffusion *per se* as a purely quantum-mechanical phenomenon is independent of the temperature. The temperature-dependent averaging of the dipolar couplings only enters indirectly by reducing the effective coupling constant.

The situation is less clear in the proximity of the glass transition temperature T_g, where displacements by Brownian segment diffusion start to freeze in. At the same time, dipolar couplings are no longer averaged out efficiently, and flip-flop spin diffusion becomes the dominant process. At any rate, the measuring conditions relevant for temperatures T near the glass transition do not permit investigations using the field-gradient NMR diffusometry technique. The conditions under which flip-flop spin diffusion can be detected in polymers using this method therefore are restricted to $t > \tau_{ff}$, $T > T_g$, and $M \gg M_c$.

Under such conditions it is obvious that flip-flop spin diffusion is a phenomenon that may partly conceal the true Brownian type of segment diffusion for long diffusion times. This might give rise to misinterpretations of experimental FGD data. However, the characteristics of the flip-flop spin diffusion effect itself imply informations on the type of chain dynamics. The purpose of our study therefore is to take flip-flop spin diffusion explicitly into account in the evaluation of FGD experiments, and to draw conclusions based on seg-

ment as well as flip-flop spin diffusion concerning the type of chain dynamics.

As a multiple-particle problem there is no straightforward theory of chain dynamics in entangled-polymer systems starting from first principles. Basically there are two approaches dealing with the influence of the ''matrix'' on the dynamics of a ''tagged'' polymer chain when the molecular weight is above the critical value. In the tube/reptation concept and its refinements [4–9], entanglement effects are illustratively accounted for by introducing a fictitious ''tube'' that is to represent the matrix. On the other hand, so-called renormalized Rouse formalisms as typical representatives of memory-function-type theories describe entangled-chain dynamics on a purely analytical basis [11–19]. The memory function is based on the ''projected dynamics,'' which is unknown. Thus, assumptions have to be made again. The reptation model as well as the memory function formalisms unavoidably imply intuitive elements that cannot be proven or derived on a theoretical basis. At the present state of the art, the lacking information can only be specified empirically using suitable experimental data. In the following, we will analyze the influence of Brownian segment diffusion and flip-flop spin diffusion on FGD data measured in diverse entangled polyethyleneoxide melts. As experimental parameters, the diffusion time, the molecular weight, and the degree of dilution with deuterated polymers of the same chemical species will be considered.

II. EXPERIMENTAL SECTION

A. Samples

Two undeuterated polyethyleneoxide (PEO_H) samples were studied. The specifications are as follows: (a) weight average molecular mass $M_w = 438\,000$, polydispersity $M_w/M_n < 1.2$, producer Polymer Standard Service, and (b) $M_w = 5\,000\,000$, $M_w/M_n < 1.2$, Aldrich. In addition, a mixture of 15.2% PEO_H 438 000 and 84.8% deuterated polyethyleneoxide PEO_D ($M_w = 460\,000$, $M_w/M_n = 1.4$, Polymer Standard Service) was investigated. The degree of deuteration of the deuterated polymer was 99%.

The polymers were first dissolved in chloroform (typically 0.5 g/100 ml). In order to make sure that complete equilibrium was reached, the PEO_H solutions were stored for more than 2 days, and the PEO_H/PEO_D mixture for 2 weeks. The solutions were then inspissated at room temperature so that a thin solid polymer film was produced at the surface of the sample container. After evacuation first at room temperature and later at 80 °C in vacuum better than 10^{-6} bar for 24 h, the samples were sealed in NMR tubes under nitrogen atmosphere in order to prevent degradation by oxygen. Size exclusion chromatography control measurements of the molecular weight distribution were carried out before and after the preparation procedure and the diffusometry experiments. No changes could be detected, so that degradation of the polymers can be excluded. PEO 5 000 000 was already investigated in our previous study [20]. However, in later control tests it turned out, that sample had degraded somewhat, so that the long-time effective diffusion coefficient was about twice as high as found with fresh samples in the present study where degradation can safely be ruled out.

The crystallization temperature range of our samples was checked with differential scanning calorimetry. It turned out that crystallization of the material can safely be excluded above 65 °C. All diffusion measurements were performed at 80 °C, i.e., well above the nominal melting temperature of 61 °C. The sample temperature was controlled with an accuracy of better than ±1 °C.

B. Measuring technique

Diffusion was studied with the aid of the fringe field variant of field-gradient NMR diffusometry as described in our previous study [2]. The stimulated (stim.) echo was recorded using the standard radio frequency (rf) pulse sequence

$$\frac{\pi}{2}\text{-}\tau_1\text{-}\frac{\pi}{2}\text{-}\tau_2\text{-}\frac{\pi}{2}\text{-}\tau_1\text{-(stim. echo)}, \tag{1}$$

in the presence of the steady fringe field gradient of a 9.4-T magnet with a 8.9-cm room-temperature bore. The gradient was $G = 60$ T/m at 200 MHz proton resonance frequency. The 90° pulse width achieved at ~300 W rf power typically was 1.6 μs. The magnet and the probehead were screened from building vibrations by air-inflated damping units. The sample was mounted in the probe without mechanical contact to the rf coil.

In the nomenclature usual with the pulsed gradient spin echo diffusometry variant, the relevant time intervals are $\tau_1 = \delta$ and $\tau_1 + \tau_2 = \Delta$. The pulse interval τ_1, that is, the ''wave number'' $q = \gamma G \tau_1$, γ is the gyromagnetic ratio, was varied while τ_2 was taken as an experimental parameter. In all cases, it was made sure that $\tau_2 \gg \tau_1$ (or $\Delta \gg \delta$), so that the diffusion time may be equated with the second pulse interval, $t = \Delta \approx \tau_2$.

The attenuation of the stimulated-echo amplitude as a function of the pulse intervals is determined by several factors according to [1]

$$A_G = A_{r2}(2\tau_1)A_{r1}(\tau_2)A_{dc}(2\tau_1)A_d(\tau_1,\tau_2). \tag{2}$$

The attenuation factors A_{r2}, A_{r1}, A_{dc}, and A_d are due to transverse relaxation (i.e., contribution of the component subject to motional averaging), spin-lattice relaxation, the dipolar-correlation effect (DCE), and translational diffusion, respectively.

As dipolar coupling was not averaged out completely under the experimental conditions of this study, the dipolar correlation effect [21,22] had to be taken into account in the analysis of the diffusive attenuation factor. In a separate experiment, the echo attenuation was therefore comparatively determined in the homogeneous central field of a Bruker Biospec magnet at the same frequency and pulse intervals, and using the same rf electronic console. In this case, diffusive attenuation does not occur, and the total attenuation of the stimulated echo is given by

$$A_{hom}(\tau_1,\tau_2) = A_{r2}(2\tau_1)A_{r1}(\tau_2)A_{dc}(2\tau_1). \tag{3}$$

Forming the quotient of the attenuation factors at Eqs. (2) and (3),

$$\frac{A_G(\tau_1,\tau_2)}{A_{hom}(\tau_1,\tau_2)}=A_d(\tau_1,\tau_2), \tag{4}$$

then provides the true attenuation factor for translational diffusion corrected for relaxation and DCE effects.

III. THEORETICAL BACKGROUND

A. Anomalous segment diffusion

Let τ_{max} be the longest correlation time of the chain conformation. In the tube/reptation model this time constant is called the ''tube disengagement'' time. Then, it becomes clear that for $t \gg \tau_{max}$ diffusion is unrestricted, and the mean squared displacement of the center of mass of the chain follows the linear Einstein relationship. On a shorter time scale, however, displacements of segments rather than of the center of mass have to be considered. This ''segment diffusion'' generally tends to show anomalous mean squared displacement laws. That is, power laws of the type

$$\langle r^2(t)\rangle \propto b^2 N^{-\alpha}\left(\frac{t}{\tau_s}\right)^{\beta} \tag{5}$$

are expected, where b is the Kuhn segment length, and N is the number of Kuhn segments per chain. The local Kuhn segment correlation time is designated by τ_s. The exponents α and β depend on the limiting case of the model considered. For example, the reptation model [5] suggests the exponents $\alpha=0$ and $\beta=1/4$ in the limit $\tau_e \ll t \ll \tau_R$ (limit II), the exponents $\alpha=1/2$ and $\beta=1/2$ for $\tau_R \ll t \ll \tau_d$ (limit III), and the exponents $\alpha=2$ and $\beta=1$ for $t \gg \tau_d$ (limit IV), where τ_e, τ_R, and τ_d are the ''entanglement,'' ''Rouse relaxation,'' and ''disengagement times,'' respectively.

B. Flip-flop spin diffusion

Flip-flop spin diffusion is traditionally considered in context with solids where dipolar interaction is not averaged out by molecular motion [23]. Under such conditions, the spin diffusion coefficient is estimated to be of the order 10^{-16} m^2/s. In low viscous liquids, on the other hand, where motional averaging of short-range dipolar interactions is complete, spin diffusion is expected to be totally negligible relative to Brownian particle motion. Neither of these situations applies to macromolecular liquids. Rather, the combined action of Brownian segment diffusion and spin flip-flop processes leads to displacements that are well in the measurable range [2,24,25].

The mean time τ_{ff} a spin flip-flop process takes in polymers is in the order [2] of 100 ms. During this time, the spins participating in the flip-flop process diffuse a distance on the order of 25 nm away by ordinary segment motions, given that they are sitting on segments of different chains. That is, an effective flip-flop spin diffusion coefficient D_{ff} in the order of 10^{-15} m^2/s is expected, which is safely within the accessible measuring range [2].

C. Spin-echo attenuation by reptation

In Ref. [26] an evaluation formalism for NMR diffusometry experiments anticipating the validity of the reptation model was presented. The resulting echo attenuation factor is

$$A_d(q^2,t)=\exp\left\{\frac{q^4a^2\langle s^2(t)\rangle}{72}\right\}\operatorname{erfc}\left\{\frac{q^2a\sqrt{\langle s^2(t)\rangle}}{6\sqrt{2}}\right\} \times \exp\{-q^2D_{cm}t\}, \tag{6}$$

where the mean squared curvilinear displacement along the tube is given by [5]

$$\langle s^2(t)\rangle=\frac{2D_0t}{N+\dfrac{12a^2D_0t}{N^2b^4}}+\frac{2b\sqrt{D_0t}}{\sqrt{3\pi}+18\dfrac{\sqrt{D_0t}}{Nb}} =\frac{6\langle R^2\rangle D_{cm}t}{a^2\left(1+\dfrac{36D_{cm}t}{\langle R^2\rangle}\right)}+\frac{2\langle R^2\rangle\sqrt{3D_{cm}t}}{a\sqrt{3\pi}+18\sqrt{3D_{cm}t}}. \tag{7}$$

The mean step length of the primitive path,

$$a=\sqrt{M_e\frac{\langle R^2\rangle}{M_w}}, \tag{8}$$

is expressed as a function of the mean squared chain end-to-end distance divided by the molecular weight. The so-called segment diffusion coefficient is defined by

$$D_0=\frac{k_BT}{\zeta}, \tag{9}$$

where ζ is the segmental friction coefficient. The center-of-mass diffusion coefficient,

$$D_{cm}=\frac{a^2k_BT}{3N^2b^2\zeta}=\frac{a^2D_0}{3N^2b^2}, \tag{10}$$

can be related to a known reference value, D_{ref}, of a sample of the same polymer species with a molecular weight M_{ref} by

$$D_{cm}=D_{ref}\left(\frac{M_{ref}}{M_w}\right)^2, \tag{11}$$

where the well-known square molecular weight dependence predicted by the reptation model is implied.

Equations (6) and (7) in this form do not yet account for the influence of flip-flop spin diffusion. Therefore its validity is restricted to diffusion times shorter than the mean flip-flop time, which for polyethyleneoxide is in the order of 100 ms (see Ref. [2]). However, the range of validity can be extended to longer times by replacing the Brownian center-of-mass diffusion coefficient D_{cm} by an apparent center-of-mass diffusion coefficient,

$$D_{cm}^{app}=D_{cm}+D_{ff}, \tag{12}$$

which is supplemented by the independent flip-flop spin diffusion coefficient D_{ff} (see below).

D. The effective segment diffusion coefficient

The evaluation and discussion of experimental data can be facilitated by considering the effective, time-dependent diffusion coefficient instead of considering the full attenuation curve based on Eq. (6) and the time-independent segment and center-of-mass diffusion coefficients defined before. In the limit of long diffusion times relative to the encoding gradient intervals, $t \gg \tau_1$, the echo attenuation by diffusion can be represented by

$$A_d(q,t) = \langle \exp\{iqz(t)\} \rangle. \tag{13}$$

In fringe field experiments, the field gradient is directed along the z axis. The displacement component along the gradient direction is represented by $z(t)$, the ''wave number'' by $q = \gamma G \tau_1$, where γ is the gyromagnetic ratio, G is the gradient strength. The brackets in Eq. (13) indicate the ensemble average formed with the aid of the probability density for displacements $z(t)$ in the diffusion time t (which essentially is equal to the pulse interval τ_2 under the present conditions). No assumption concerning a potentially Gaussian character of this probability density is made. Expanding Eq. (13) and taking the limit for small q values leads to the approximate expressions

$$A_d(q,t) \approx 1 - \frac{q^2}{2}\langle z^2(t) \rangle \approx \exp\left\{ -\frac{q^2}{2}\langle z^2(t) \rangle \right\} = \exp\left\{ -\frac{q^2}{6}\langle r^2(t) \rangle \right\}. \tag{14}$$

The exponent is obviously dominated by the second moment of the probability density. Formally equating this quantity with the result expected for a Gaussian probability density leads to

$$\langle r^2(t) \rangle = 6\tilde{D}t, \tag{15}$$

where $\tilde{D}$ is the effective and, according to Eq. (5), time-dependent diffusion coefficient that is defined in this way. The echo attenuation function can then be rewritten for small q values as

$$A_d(q,t) \approx \exp\{-q^2 \tilde{D} t\}. \tag{16}$$

That is, plots of $\ln A_d(q,t)$ versus q^2 are expected to reveal straight lines in the limit of sufficiently small q values. Note however, that the attenuation curves deviate from straight lines at large wave numbers whenever the probability density deviates from a Gaussian distribution.

E. Evaluation formulas for the effective diffusion coefficient

The effective diffusion coefficient evaluated in the small wave-number limit accounts for all time-dependent and -independent contributions of Brownian diffusion or flip-flop spin diffusion to segment or center-of-mass displacements. Analogous to the center-of-mass diffusion coefficient, Eq. (12), an overall effective diffusion coefficient $\tilde{D}$ can be defined consisting of two contributions,

$$\tilde{D}(t) = D_{ff} + D_{tr}(t), \tag{17}$$

where $D_{tr}(t)$ describes translations of the spin-bearing nuclei. The time dependence refers to the anomalous segment diffusion regime, Eq. (5), of course.

The contribution by segment diffusion was shown to obey [25]

$$D_{tr}(t) = \frac{At^\beta}{6} e^{-t/\tau_{ff}} \left(\frac{1}{t} + \frac{1}{\tau_{ff}} \right) + \frac{A\tau_{ff}^\beta}{6} \left(\frac{1}{\tau_{ff}} + \frac{1-\beta}{t} \right) \times \gamma\left(\beta + 1; \frac{t}{\tau_{ff}} \right) \tag{18}$$

$$= \frac{At^{\beta-1}}{6} e^{-t/\tau_{ff}} \Gamma(1+\beta) \sum_{k=0}^{\infty} \frac{1+k}{\Gamma(1+\beta+k)} \times \left(\frac{t}{\tau_{ff}} \right)^k, \tag{19}$$

where A is defined as a proportionality constant in the law $\langle r^2 \rangle = At^\beta$. $\gamma(x,y)$ is the incomplete gamma function and $\Gamma(x)$ is the ordinary gamma function. The flip-flop spin diffusion coefficient is described [25] by

$$D_{ff} = \left(\frac{\mu_0}{4\pi} \right)^2 \frac{16\sqrt{6\pi}\,\Gamma(\frac{5}{9})}{315\sqrt{2}} \frac{\gamma^4 \hbar^2 \rho_s T_2}{\sqrt{\langle r^2(T_2) \rangle}} \tag{20}$$

as a function of the mean-squared segment displacement $\langle r^2(T_2) \rangle$ during the transverse relaxation time T_2. The spin number density is represented by ρ_s. Equations (18) and (20) are based on the mean squared spin displacements and the corresponding parameters.

On the other hand, the mean-squared displacement for the reptation model can be approximated for times longer than the segment relaxation time by [26]

$$\langle r^2(t) \rangle_{rept} = 6D_{cm}t + \sqrt{\frac{2}{\pi}} a \sqrt{\langle s^2(t) \rangle}, \tag{21}$$

where $\langle s^2(t) \rangle$ is to be taken from Eq. (7).

It turned out that in the transition region from anomalous diffusion to ordinary center-of-mass diffusion the description of the mean squared segment displacement by power laws was not accurate enough to approximate the behavior of the polymer segments in this time interval. The mean squared displacement, therefore, has been calculated by numerically evaluating the sum in the expression that is valid for limits [5] III and IV of the tube/reptation model,

$$\langle r^2(t) \rangle_{\mathrm{III/IV}} = 6D_{cm}t + \frac{\langle R^2 \rangle}{3\pi^2 t} \sum_{p=1}^{\infty} \times \frac{1}{p^2} [1 - \exp\{-3\pi^2 p^2 \langle R^2 \rangle / (D_{cm}t)\}]. \tag{22}$$

IV. VALUES OF THE FIXED PARAMETERS

The evaluation formulas given in Eqs. (18)–(22) depend on a number of parameters that partly can be estimated from known literature data. Choosing a reference molecular mass

in a range where anomalous segment diffusion and flip-flop spin diffusion do not affect the experiments, $M_{ref}=12\,300$, but still well above the critical molecular mass of [27] $M_C=3600$, permits us to extrapolate the center-of-mass diffusion coefficient, D_{cm}, at our molecular masses and temperatures based on data given in Refs. [28–30] and using Eq. (11). For 80 °C the reference self-diffusion coefficient is determined as $D_{ref}=3.1\times10^{-13}$ m^2/s.

The flip-flop spin diffusion coefficient, D_{ff} is estimated on the basis of Eq. (20). With $\gamma=2.6752\times10^{8}$ (T s)$^{-1}$, $\hbar=1.0546\times10^{-34}$ J s, $\mu_0=1.2566\times10^{-6}$ H/m and $\Gamma(\frac{5}{9})=1.60$ we obtain

$$D_{ff}=2.0098\times10^{-49}\frac{\mathrm{m}^6}{\mathrm{s}^2}\frac{\rho_s T_2}{\sqrt{\xi\langle r^2(T_2)\rangle}}. \tag{23}$$

The parameter ξ represents any potential correlation in the dynamics of neighboring chains. It takes the value 2 for independent segment displacements. This will tentatively be anticipated in the following.

The transverse relaxation T_2 has been determined for each of the investigated samples in separate measurements in a homogeneous magnetic field at the same rf frequency and at the same temperature. The results are $T_2=2.0$, 2.5, and 1.8 ms for PEO_H $M_w=438\,000$ (bulk), 438 000 (15.2% in deuterated matrix), and 5 000 000, respectively. The spin number density of bulk polyethyleneoxide can be estimated as $\rho_s\approx6\times10^{28}$ m^{-3}. Note that the deuterated matrix contains about 1% residual protons, so that the spin number density in the isotopically diluted sample consisting of 15.2% undeuterated material in a matrix with a deuteration degree of 99% is related to the value in the undiluted samples by the factor $15.2\%+84.8\%\times1\%=0.1605$. All other parameters can be expressed as functions of the parameters discussed so far.

Thus, the only remaining free fitting parameter is the mean squared chain end-to-end distance divided by the molecular mass,

$$\sigma\equiv\langle R^2\rangle/M_w. \tag{24}$$

It is generally accepted that this quantity does not depend on the molecular mass. Therefore the mean squared chain end-to-end distance for any molecular mass can be calculated via

$$\langle R^2\rangle=M_w\sigma. \tag{25}$$

Likewise, the mean step length of the primitive path a can be expressed by this characteristic ratio and the critical molecular mass [27], $M_c=3600$,

$$a=\sqrt{\frac{M_c}{2}\sigma}. \tag{26}$$

The coil dimension data derived from the present investigation are compared with the findings of neutron scattering experiments [31] carried out with a polyethyleneoxide melt, $M_w=100\,000$, $M_w/M_n=1.5$, at 80 °C. In that study, a value $\sigma=1.01\times10^{-20}$ m^2 mol/g was found. In a more recent neutron scattering investigation [32] on a polyethyleneoxide fraction with narrow molecular weight distribution ($M_W=110\,000$, $M_w/M_n=1.01$) a somewhat lower value, $\sigma=0.83\times10^{-20}$ m^2 mol/g was obtained.

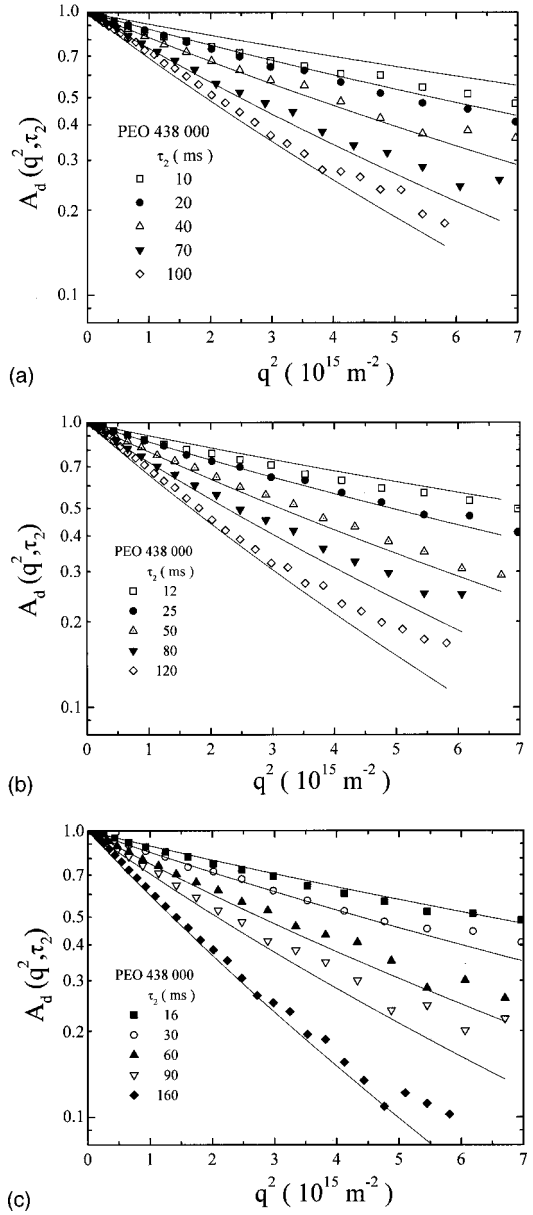

FIG. 1. Decays of the stimulated-echo amplitude of PEO 438 000 melts at 80 °C due to attenuation by segment and flip-flop spin diffusion. The abscissa axes refer to the squared wave number ($q=\gamma G\tau_1$). The curve parameter is the diffusion interval τ_2. The solid lines in (a), (b), and (c) represent fits of Eqs. (6), (7), and (12). Predetermined parameters were $D_{ref}=3.1\times10^{-13}$ m^2/s, $M_{ref}=12\,300$, $M_c=3600$, $\rho_s=6\times10^{28}$/m^3, $T_2=2.0$ ms. The fitted parameter is $\sigma=(4.5\pm0.4)\times10^{-20}$ m^2 mol/g.

This difference was attributed to the slightly higher polydispersity of the sample used in Ref. [31]. As the polydispersity of our samples is more like the one in Ref. [31], we take $\sigma=1.01\times10^{-20}$ m^2 mol/g as a reference value.

V. RESULTS

Figures 1 and 2 show typical echo attenuation data as a function of the squared wave number. The curve parameter is the diffusion time τ_2. Anticipating the validity of the repta-

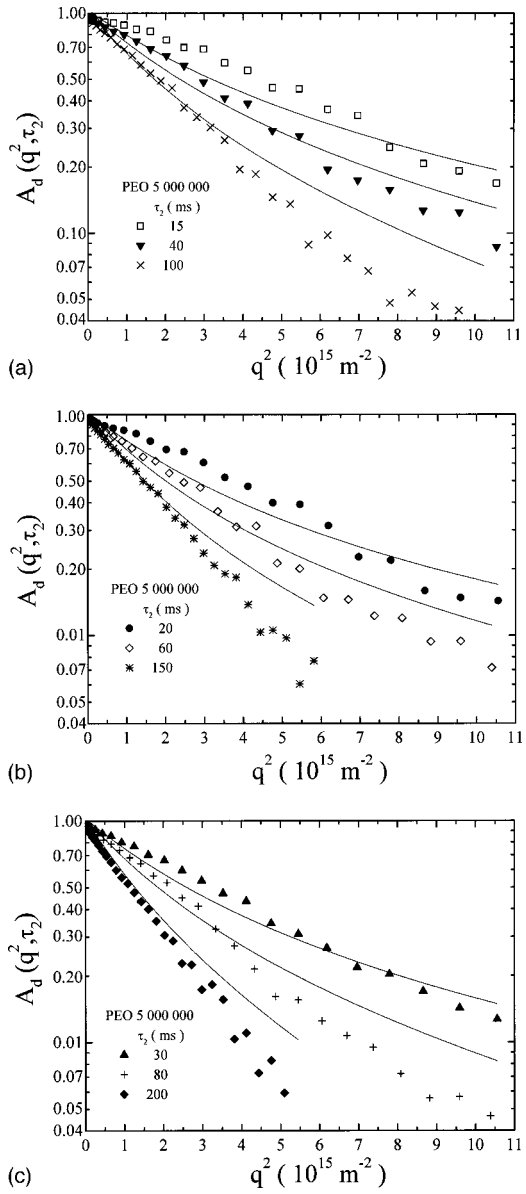

FIG. 2. Decays of the stimulated-echo amplitude of PEO 5 000 000 melts at 80 °C due to attenuation by segment and flip-flop spin diffusion. The abscissa axes refer to the squared wave number ($q=\gamma G\tau_1$). The curve parameter is the diffusion interval τ_2. The solid lines in (a), (b), and (c) represent fits of Eqs. (6), (7), and (12). Predetermined parameters were $D_{ref}=3.1\times10^{-13}$ m^2/s, $M_{ref}=12\,300$, $M_c=3600$, $\rho_s=6\times10^{28}$/m^3, and $T_2=1.8$ ms. The fitted parameter is $\sigma=(2.5\pm0.4)\times10^{-19}$ m^2 mol/g.

tion model, Eq. (6) was fitted to the data sets for polyethyleneoxide $M_w=438\,000$ and $M_w=5\,000\,000$, considering the displayed data for all diffusion times for each sample together at one time. The influence of flip-flop spin diffusion was taken into account according to Eqs. (12) and (20). The only free fitting parameter was $\sigma\equiv\langle R^2\rangle/M_w$.

For the lower molecular mass, reasonable agreement of the fitted curves with the data can be stated. This is in contrast to the sample with the high molecular mass. Moreover, the values obtained for the fitting parameter $\langle R^2\rangle/M_w$ turned out to be unrealistically large. The results are $(4.5\pm0.4)\times10^{-20}$ m^2 mol/g and $(2.5\pm0.4)\times10^{-19}$ m^2 mol/g for PEO 438 000 and PEO 5 000 000, respectively. That is, the discrepancy to the neutron scattering value [31] is a factor of 4.5 and 25, respectively.

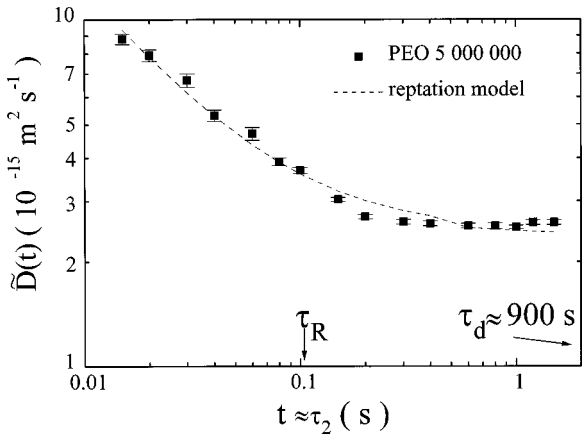

FIG. 3. Effective diffusion coefficient of polyethyleneoxide $M_w=5\,000\,000$ at 80 °C as a function of the diffusion time $t\approx\tau_2$. The solid lines represent fits of Eqs. (17), (18), and (20) with τ_{ff} and σ as the only fitting parameters ($\xi=2$). For the reptation model one obtains $\tau_{ff}=(0.12\pm0.02)$ s and $\sigma=(8.1\pm0.4)\times10^{-20}$ m^2 mol/g.

At diffusion times longer than the mean flip-flop time, a substantial contribution by flip-flop spin diffusion becomes obvious. Figures 3 and 4 show proton data of the effective diffusion coefficient measured in PEO 5 000 000 and PEO 438 000, respectively, as a function of the diffusion time on the basis of Eq. (16). In order to demonstrate the effect of flip-flop spin diffusion, Fig. 4 also shows data for polymer chains in a deuterated matrix of an equivalent molecular mass. That is, the interchain dipolar interaction is strongly reduced in this case, and, hence, the intermolecular spin flip-flop rate as well.

The time-independent plateau of the effective diffusion coefficient of PEO 5 000 000 appearing at long diffusion times (Fig. 3) certainly cannot be due to center-of-mass diffusion. Apart from the absolute value of the diffusion coef-

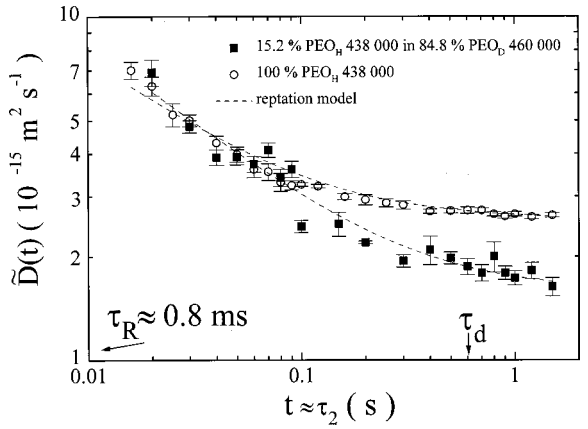

FIG. 4. Effective diffusion coefficient of polyethyleneoxide $M_w=438\,000$ in bulk and diluted in a deuterated matrix at 80°C as a function of the diffusion time $t\approx\tau_2$. The dashed lines represent fits of Eqs. (17), (18), (20), and (22) for the reptation model ($\xi=2$). The results for the bulk sample are $\tau_{ff}=(0.11\pm0.01)$ s and $\sigma=(4.5\pm0.5)\times10^{-20}$ m^2 mol/g. For PEO$_H$ in deuterated matrix we find $\tau_{ff}=(0.27\pm0.03)$ s, $\sigma=(6\pm1)\times10^{-20}$ m^2 mol/g.

TABLE I. Fitted parameter values and calculated $D_{ff}(\xi=2)$.

M_w	τ_{ff}/s	$\sigma/(10^{-20}$ m^2 mol/g)	$D_{ff}/$(m^2/s)
438 000 (bulk)	(0.11 ± 0.01)	(4.5 ± 0.5)	9.9×10^{-16}
438 000 (15.2%)	(0.27 ± 0.03)	(6 ± 1)	1.7×10^{-16}
5 000 000 (bulk)	(0.12 ± 0.02)	(8.1 ± 0.4)	7.3×10^{-16}

ficient, which is by orders of magnitude larger than the center-of-mass diffusion coefficient expected for this molecular weight, the investigated time scale is far below the longest chain relaxation time. In the frame of the reptation model, for example, one estimates a tube disengagement time of $\tau_d\approx900$ s, whereas the plateau starts already at 200 ms. That is, the only explanation of the plateau value and its extension to short diffusion times is flip-flop spin diffusion.

This conclusion is corroborated by the fact that isotopic dilution by deuterated chains reduces the plateau value (Fig. 4). The data for PEO 438 000 in a deuterated matrix actually approach the true plateau value expected in the absence of flip-flop spin diffusion: The tube disengagement time is estimated in this case to be 0.6 s, i.e., well within the accessible time scale.

The dashed lines in Figs. 3 and 4 represent fits of Eqs. (17), (18), and (20) for the reptation model specified by the mean squared segment displacement according to Eq. (21) and Eq. (22), respectively. The flip flop time τ_{ff} and $\sigma\equiv\langle R^2\rangle/M_w$ are the only fitting parameters; all other parameters are predetermined from other information sources as outlined above. For PEO 5 000 000, we find $\tau_{ff}=(0.12\pm0.02)$ s, $\langle R^2\rangle/M_w=(8.1\pm0.4)\times10^{-20}$ m^2 mol/g. The fitted parameter values for PEO 438 000 are $\tau_{ff}=(0.11\pm0.01)$ s, $\sigma=(4.5\pm0.5)\times10^{-20}$ m^2 mol/g for the bulk sample, and $\tau_{ff}=(0.27\pm0.03)$ s, $\sigma=(6\pm1)\times10^{-20}$ m^2 mol/g for PEO_H in the deuterated matrix. The σ values are again larger than the neutron scattering value [31]. In Table I the fitting results corresponding to Figs. 3 and 4 are listed for comparison. In addition, the spin diffusion coefficient has been calculated based on the σ values.

VI. CONCLUSIONS AND DISCUSSION

Field gradient NMR diffusion measurements probe chain dynamics of sufficiently long polymers in a range where anomalous segment diffusion dominates. The method is therefore suitable for testing corresponding model predictions. In particular it should be noted that the diffusion time scale ranges from milliseconds up to the order of seconds, i.e., to a scale inaccessible to other techniques such as radioactive tracer and quasielastic neutron scattering experiments. In this study we have concentrated on the ability of the tube/reptation model to describe the anomalous diffusion behavior as revealed by the fringe-field NMR diffusometry technique.

In evaluating experimental data two important implications must be taken into account. First, anomalous diffusion of polymer segments requires a model-dependent modification of the usual evaluation formulas for field gradient NMR diffusion measurements [see Eqs. (6) and (7)] unless an effective diffusion coefficient [see Eq. (16)] is considered for small q values. Second, at diffusion times longer than the intermolecular spin flip-flop time τ_{ff}, which is on the order of 100 ms, immaterial spin diffusion starts to dominate the effective diffusion coefficient.

The effective diffusion coefficient data of PEO 5 000 000 and PEO 438 000 melts reported here clearly demonstrate the influence of this intermolecular flip-flop spin diffusion. The effect is further substantiated by an isotopic dilution effect on the diffusion data. The echo attenuation curves can hence be evaluated on the basis of Brownian segment diffusion alone only for diffusion times shorter than the mean intermolecular spin flip-flop time $\tau_{ff}\approx100$ ms.

The time dependences of the effective diffusion coefficient were compared with the expectations on the basis of the reptation model. The combined effect of flip-flop spin diffusion and Brownian segment diffusion was taken into account. The fitted values for the mean squared chain end-to-end distance relative to the molecular weight, $\langle R^2\rangle/M_w$ turned out to be much larger than those concluded from neutron scattering experiments.

This discrepancy becomes plausible when considering the intuitive assumptions of the tube/reptation model for liquid entangled polymers: The diameter of the tube is considered as free fitting parameter. When fitted to plateau modulus data of mechanical relaxation, values on the order of 5–10 nm come out that are one order of magnitude larger than the mean distance of neighboring chains. Within the tube on a length scale of its diameter, the validity of the Rouse model originally derived for free chains in a viscous medium is anticipated. That is, the numerous polymer chains filling the space inside the tube are assumed to cross each other without any excluded-volume restrictions. Because this scenario is intrinsically unrealistic, the model predictions in the anomalous segment diffusion regime unavoidably are subject to overestimations. The situation would certainly become more favorable for the reptation model if the time scale above the tube disengagement time could be considered. With the molecular masses and the investigation method of the present study, this time scale is, however, far from being accessible.

In this context, it is of interest that the confinement of polymer chains into pore channels of a diameter much less than the coil diameter in bulk more closely corresponds to the presumptions of the reptation model anticipating ''fixed obstacles'' as topological constraints of chain dynamics [4]. NMR experiments carried out under such conditions do reproduce the specific predictions of the model indeed [29,10].

The tube/reptation model is difficult to modify for chain-chain interactions and correlations more refined than just the tube hypothesis. The reason is the purely geometrical nature of this ansatz. An analytical treatment from the very beginning may be superior in this respect. Unfortunately no theory starting from first principles is available due to the many-particle character of the problem. That is, any purely analytical approach unavoidably will be subject to intuitive assumptions that have to be incorporated into the formalism. The advantage may however be that modifications of these assumptions can easily be performed in order to achieve better coincidence with experimental data.

It is clear that the ordinary Rouse model cannot account for the experimental findings of this study: The molecular-mass and time dependences as well as the absolute values of the effective diffusion coefficients predicted on this basis are incompatible with our data. However, as already mentioned

in the introductory section, versions extended in the form of memory function formalisms could be exploited in this context [11–19]. In this case, the main objective is to reveal limiting cases of the chain dynamics on the basis of a generalized Langevin equation of motion. While the limiting-case structure as such may correctly be represented by the results, the remaining arbitrary element of this formalism is the intuitive basis of the memory function that has to be assumed. This particularly refers to absolute values of the parameters and to the exponent values of power laws. A semiempirical theory of this sort nevertheless may be useful for the solution of the polymer dynamics problem. A corresponding treatment will be published elsewhere.

ACKNOWLEDGMENTS

This work was supported by the Volkswagen-Stiftung, the Deutsche Forschungsgemeinschaft, and RFFI (Grant No. 98-03-33307a). We thank Dr. U. Beginn and G. Hanich for the SEC/GPC characterization of the polymer samples and for helpful discussions.

[1] R. Kimmich, *NMR: Tomography, Diffusometry, Relaxometry* (Springer, Berlin, 1997).
[2] E. Fischer, R. Kimmich, and N. Fatkullin, J. Chem. Phys. **106**, 9883 (1997).
[3] M. E. Komlosh and P. T. Callaghan, J. Chem. Phys. **109**, 10 053 (1998).
[4] P. G. de Gennes, J. Chem. Phys. **55**, 572 (1971).
[5] M. Doi and S. F. Edwards, *The Theory of Polymer Dynamics* (Clarendon, Oxford, 1986).
[6] M. Doi, Polym. Sci. Lett. **19**, 265 (1981).
[7] M. Rubinstein, Phys. Rev. Lett. **59**, 1946 (1987).
[8] W. W. Graessley, Adv. Polym. Sci. **47**, 67 (1982).
[9] S. T. Milner and T. C. B. McLeish, Phys. Rev. Lett. **81**, 725 (1998).
[10] R. Kimmich, R.-O. Seitter, U. Beginn, M. Möller, and N. Fatkullin, Chem. Phys. Lett. **307**, 147 (1999).
[11] G. Ronca, J. Chem. Phys. **79**, 1031 (1983).
[12] M. Fixman, J. Chem. Phys. **89**, 3892 (1988).
[13] J. Skolnick and A. Kolinski, Adv. Chem. Phys. **78**, 223 (1990).
[14] J. F. Douglas and J. B. Hubbard, Macromolecules **24**, 3163 (1991).
[15] M. F. Hermann, Macromolecules **25**, 4925 (1993).
[16] A. P. Chatterjee and R. F. Loring, J. Chem. Phys. **1995**, 4711 (1995).
[17] K. S. Schweizer, J. Chem. Phys. **91**, 5802 (1989).
[18] K. S. Schweizer, J. Chem. Phys. **91**, 5822 (1989).
[19] K. S. Schweizer, M. Fuchs, G. Szamel, M. Guenza, and H. Tang, Macromol. Theory Simul. **6**, 1037 (1997).
[20] E. Fischer, R. Kimmich, and N. Fatkullin, J. Chem. Phys. **104**, 9174 (1996).
[21] R. Kimmich, E. Fischer, P. T. Callaghan, and N. Fatkullin, J. Magn. Reson., Ser. A **117**, 53 (1995).
[22] F. Grinberg and R. Kimmich, J. Chem. Phys. **103**, 365 (1995).
[23] M. Goldman, *Spin Temperature and Nuclear Magnetic Resonance in Solids* (Clarendon Press, Oxford, 1970).
[24] N. F. Fatkullin, Zh. Éksp. Teor. Fiz. **99**, 1013 (1991) [Sov. Phys. JETP **72**, 563 (1991)].
[25] N. F. Fatkullin, G. Yatsenko, R. Kimmich, and E. Fischer, Pis'ma Zh. Éksp. Teor. Fiz. **114**, 538 (1998) [JETP **87**, 294 (1998)]; N. Fatkullin, thesis (second dissertation), University of Kazan, 1995.
[26] N. Fatkullin and R. Kimmich, Phys. Rev. E **52**, 3273 (1995).
[27] W. W. Graessley and S. F. Edwards, Polymer **22**, 1329 (1981).
[28] M. Appel and G. Fleischer, Macromolecules **26**, 5520 (1993).
[29] E. Fischer, R. Kimmich, U. Beginn, M. Moeller, and N. Fatkullin, Phys. Rev. E **59**, 4079 (1999).
[30] A. I. Maklakov, V. D. Skirda, and N. F. Fatkullin, in *Encyclopedia of Fluid Mechanics, Vol. 9: Polymer Flow Engineering*, edited by N. P. Cheremisinoff (Gulf, Houston, 1990).
[31] J. Kugler and E. W. Fischer, Makromol. Chem. **184**, 2325 (1983).
[32] G. D. Smith, D. Y. Yoon, R. L. Jaffe, R. H. Colby, R. Krishnamoorti, and L. J. Fetters, Macromolecules **29**, 3462 (1996).